

See discussions, stats, and author profiles for this publication at: <https://www.researchgate.net/publication/259358415>

# Functionalization of Aluminum Nanoparticles Using a Combination of Aryl Diazonium Salt Chemistry and Iniferter Method

ARTICLE in THE JOURNAL OF PHYSICAL CHEMISTRY C · NOVEMBER 2013

Impact Factor: 4.77 · DOI: 10.1021/jp406356s

---

CITATIONS

13

READS

124

## 11 AUTHORS, INCLUDING:



Jean Pinson

Paris Diderot University

162 PUBLICATIONS 7,606 CITATIONS

[SEE PROFILE](#)



Aazdine Lamouri

Paris Diderot University

41 PUBLICATIONS 480 CITATIONS

[SEE PROFILE](#)



Jean-Yves Piquemal

Paris Diderot University

59 PUBLICATIONS 1,123 CITATIONS

[SEE PROFILE](#)



Anouk Galtayries

Chimie ParisTech

91 PUBLICATIONS 1,242 CITATIONS

[SEE PROFILE](#)

# Functionalization of Aluminum Nanoparticles Using a Combination of Aryl Diazonium Salt Chemistry and Iniferter Method

Yasmine Aït Atmane,<sup>†</sup> Lorette Sicard,<sup>\*,†</sup> Aazdine Lamouri,<sup>†</sup> Jean Pinson,<sup>†</sup> Mickaël Sicard,<sup>‡</sup> Christian Masson,<sup>‡</sup> Sophie Nowak,<sup>†</sup> Philippe Decorse,<sup>†</sup> Jean-Yves Piquemal,<sup>†</sup> Anouk Galtayries,<sup>§</sup> and Claire Mangeney<sup>\*,†</sup>

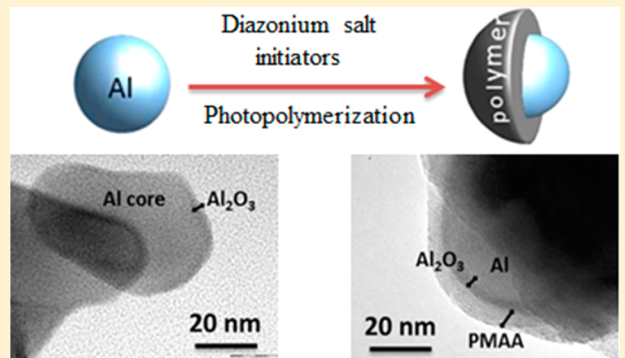
<sup>†</sup>Univ Paris Diderot, Sorbonne Paris Cité, ITODYS, UMR 7086 CNRS, 15 rue J-A de Baïf, 75205 Paris, Cedex 13, France

<sup>‡</sup>ONERA, The French Aerospace Lab, F-91123 Palaiseau, France

<sup>§</sup>Laboratoire de Physico-Chimie des Surfaces, CNRS-ENSCP (UMR 7045), Chimie ParisTech, 11 rue Pierre et Marie Curie, F-75005 Paris, France

## Supporting Information

**ABSTRACT:** In this work, we propose an original strategy for the functionalization of aluminum nanoparticles (Al NPs), based on a combination of aryl diazonium salt chemistry and the photopolymerization iniferter method. It consists in grafting coupling agents, derived from diazonium salts, at the surface of Al NPs and in initiating the photopolymerization of methacrylic acid (MAA) directly from the surface. The hybrid NPs were fully characterized using XRD, TEM, TGA, and XPS. The results show that the obtained hybrids exhibit a core-double shell structure, the metallic core being preserved while a thin natural oxide layer and a strongly anchored organic shell surround it. The controlled and living character of the photopolymerization process allowed for the control of the polymer shell thickness with the polymerization time. Interestingly, the formation of compact aryl layers derived from the diazonium salts at the surface of Al NPs appears to provide an efficient protection against oxidation.



## 1. INTRODUCTION

Noble metal nanocrystals have attracted considerable attention owing to their potential applications in fields such as catalysis, biology, and electronics.<sup>1–4</sup> Particularly, aluminum nanoparticles (Al NPs) have been the subject of extensive research during the past decade because they can be used as additives or fuel in various applications requiring high energy output.<sup>5,6</sup> The replacement of micrometer-scale aluminum powders by aluminum nanoparticles in energetic materials leads to an enhancement of the overall reactivity of the material, favorable for the target application. However, important difficulties also arise: besides the risks associated with the manipulation of highly reactive powders, one difficulty is their tendency to aggregate (to minimize their free energy), inhibiting the formation of homogeneous nanocomposites with highly dispersed NPs. Another important problem arising from the NP size decrease is the formation of a passivated oxide layer at their surface, the relative proportion of which becomes non-negligible compared to the nonoxidized metallic Al core.<sup>7</sup> This natural oxide layer can account for a large proportion of dead weight and therefore may alter the energetic properties of the particles. In order to limit the oxide thickness and minimize particle aggregation, various chemical functionalization strategies have been developed. Particularly, for the preparation of

NPs-polymer composites, bifunctional molecules have been proposed, bearing on one side a functional group able to bind to the nanoparticle surface and on the other side, an organic component that affords favorable interaction with the polymer matrix.<sup>8</sup> In consideration that the particle consists of a metallic aluminum core passivated by a thin (a few nanometers) amorphous aluminum oxide shell, the functionalization strategies which have usually been employed were based on molecules able to chemically (or physically) interact with the amorphous aluminum oxide surface.

Toward this end, various organic ligands have been used: carboxylic acids,<sup>9–11</sup> silanes,<sup>12</sup> and phosphonic acids.<sup>13–15</sup> Nevertheless, these ligands were not shown to durably protect the Al NPs from oxidation by air leading to the formation of a thick oxide layer at their surface. Therefore, it is still challenging to develop new functionalization strategies, allowing a strong protection of the Al NP surface, stable with time. In this paper, we propose to address this issue by exploring a new method for Al surface functionalization, based on the diazonium salt chemistry. Aryl diazonium salts have been shown recently to be

Received: June 27, 2013

Revised: November 9, 2013

Published: November 19, 2013



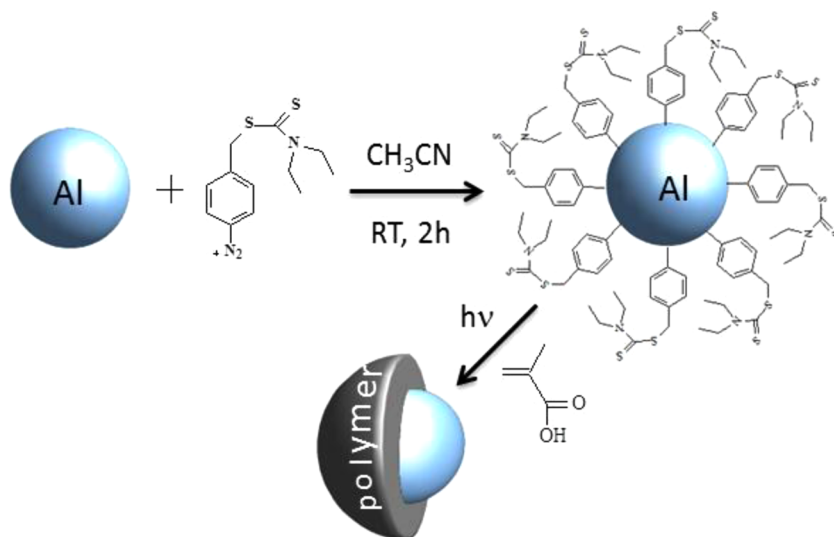


**Figure 1.** Scheme of the surface functionalization strategy of Al NPs (i) by coupling agents derived from diazonium salts, (ii) followed by photopolymerization of MAA.

useful organic agents for the surface modification of carbon-based,<sup>16–19</sup> metallic<sup>20–24</sup> (gold, platinum, palladium, ruthenium, and titanium), and oxide<sup>25–29</sup> nanoparticles, affording strong surface–carbon linkages.<sup>30–32</sup> Generally, the mechanism of these grafting reactions relies on the reduction of the diazonium salt (by the surface to modify or by a reducing agent in solution), generating aryl radical species that bind to the metal or oxide surface. Here, this strategy is used to form Al NPs coated by aryl groups with carbon–surface covalent bonds, as schematized in Figure 1. In spite of the fact that grafting of diazonium salts on metallic or oxide surfaces has already been reported, such unique chemistry has never been extended to the functionalization of Al surfaces and particularly Al nanoparticles.

As a proof of concept, we studied the functionalization of preformed Al NPs by a bifunctional initiator, 4-[(diethylcarbamothioyl)thio] methyl benzenediazonium tetrafluoroborate ( $\text{BF}_4^- \text{N}_2^+ \text{C}_6\text{H}_4\text{CH}_2\text{DEDTC}$ ), containing a diazonium end group for surface anchoring and a *N,N*-diethyldithiocarbamate (DEDTC) function able to activate surface-initiated photoiniferter-mediated polymerization (SI-PIMP).<sup>33–36</sup>

The structure, morphology, oxidation, and surface modification of the NPs were characterized by X-ray diffraction, transmission electron microscopy, thermal gravimetric analysis, and X-ray photoelectron spectroscopy.

## 2. EXPERIMENTAL SECTION

**2.1. Materials.** All the chemicals,  $\text{AlCl}_3$  (99%),  $\text{LiAlH}_4$  (97%), dried diethylether ( $\text{H}_2\text{O} \leq 0.005\%$ ), titanium(IV) isopropoxide (99.9% trace metals basis), and toluene (99.8%), were obtained from Sigma-Aldrich except absolute ethanol (Normapur) purchased from VWR. The solvents were used as received, except acetonitrile, which was dried before use. The bifunctional 4-[(diethylcarbamothioyl)thio] methyl benzenediazonium tetrafluoroborate ( $\text{BF}_4^- \text{N}_2^+ \text{C}_6\text{H}_4\text{CH}_2\text{DEDTC}$ ) was prepared following a procedure described in the literature.<sup>14</sup>

**2.2. Synthesis.** The reactions were carried out in a glovebox, under an inert atmosphere (Argon, Alphagaz 2).  $\text{LiAlH}_4$  (31.6 mmol) and  $\text{AlCl}_3$  (10.5 mmol) were both

dissolved in 15 mL of diethylether. The mixture of these two solutions resulted in the formation of  $\text{AlH}_3$  (alane), dissolved in diethylether, and  $\text{LiCl}$  which precipitates. After decantation and filtration, a solution of pure  $\text{AlH}_3$  is obtained. The addition of a catalyst, titanium isopropoxide  $\text{Ti}(\text{O}i\text{Pr})_4$ , resulted in the decomposition of  $\text{AlH}_3$  into Al and  $\text{H}_2$ . The gray powders were recovered by centrifugation and washed 3 times with diethylether. The functionalization procedure consisted simply in incubating the preformed Al NPs with the diazonium salt in acetonitrile at room temperature. In practice, 50 mg of Al powder were ground and dispersed in acetonitrile. The diazonium salt (8.3 mmol) in solution in anhydrous acetonitrile was added, and the mixture was stirred for 2 h. The particles were then centrifuged and washed by 8 cycles of dispersion in acetonitrile (using an ultrasonic bath) and centrifugation and 5 cycles using diethylether. The particles obtained are noted Al-DEDTC. The last step consisted of grafting poly(methacrylic acid) at the Al NPs surface by addition of monomers. Thirty milligrams of Al-DEDTC was dispersed in absolute ethanol and a solution containing 37.7  $\mu\text{L}$  of monomer (AM) in absolute ethanol was added. The resulting solution was placed under UV light for  $x$  (with  $x = 2, 4, 6$ , and 8) hours. The particles were washed by 8 cycles of centrifugation/redispersion in absolute ethanol under sonification. These new samples are noted Al-PMAA<sub>xh</sub>.

**2.3. Characterizations.** X-ray diffraction (XRD) patterns were recorded on a PANalytical X'Pert Pro diffractometer equipped with a Co anode [ $\lambda(\text{Co}_{\text{K}\alpha}) = 1.7903 \text{ \AA}$ ] and an X'celerator detector. The data were collected at room temperature with a  $0.026^\circ$  step size in  $2\theta$ , from  $2\theta = 20$  to  $110^\circ$ . The crystalline phase was identified by comparison with ICDD database (PDF-2). Transmission electron microscopy (TEM) characterizations were performed using a Jeol 100-CX II microscope, operating at 100 kV. The powders were first dispersed in toluene under sonication and one drop of this dispersion was deposited on a carbon grid. Scanning electron microscopy (SEM) images were obtained using a Zeiss SUPRA 40 FESEM equipped with a thermal field emission gun. Images are created using SMARTSEM. Fourier transform-infrared (FT-IR) spectra were collected on KBr pellets with a NICOLET Magna-IR 860 spectrometer in the transmittance

mode between 4000 and 650  $\text{cm}^{-1}$  with a resolution of 4  $\text{cm}^{-1}$ , 50 scans being accumulated. Thermogravimetric analysis (TGA) was performed on a Labsys evo SETARAM instrument. Samples were analyzed in an alumina pan at a heating rate of 10  $^{\circ}\text{C min}^{-1}$  from ambient temperature up to 1500  $^{\circ}\text{C}$  under air flow (18 mL min $^{-1}$ ). X-ray photoelectron spectrometry (XPS) measurements were performed using a Thermo VG Escalab 250 instrument equipped with a monochromatic Al K $\alpha$  ( $\hbar\nu = 1486.6 \text{ eV}$ ), 150–200 W microfocused X-ray source. The X-ray spot size was 500–650  $\mu\text{m}$ . The pass energy was set at 100, 40, and 15 eV for the survey, the narrow scans, and high-resolution scans, respectively. An electron flood gun was used, for static charge compensation and homogenization on isolating samples on the sample surface. These conditions resulted in a negative but uniform static charge. Measurements were carried out on powders mounted on sample holders with double-sided tape. Data acquisition and processing were performed with Avantage, version 4.67. The surface composition was determined using the integrated peak areas and the corresponding Scofield sensitivity factors corrected for the analyzer transmission function. For the majority of the compounds under study, spectra were calibrated in energy by setting (or shifting) the main C1s component, assigned to aliphatic carbons, to 285 eV. Time-of-flight secondary-ion mass spectrometry (TOF-SIMS) data were acquired using a TOF-SIMS V spectrometer (ION-TOF GmbH). The analysis chamber was maintained at less than  $5 \times 10^{-7} \text{ Pa}$  under operating conditions. The total primary ion flux was below  $10^{12} \text{ ions cm}^{-2}$  to ensure static conditions. A pulsed 25 keV Bi $^{+}$  primary ion source (Liquid Metal Ion Gun, LMIG) at a current of about 1 pA (high current bunched mode), rastered over a scan area of  $500 \times 500 \mu\text{m}$ , was used as the analysis beam.

### 3. RESULTS AND DISCUSSION

**3.1. Diffraction Patterns of Al NPs.** The native aluminum nanoparticles (sample Al) obtained by catalytic decomposition of alane, the diazonium-functionalized particles (Al-DEDTC), and the powders obtained after polymerization (Al-PMAA $_{\text{sh}}$ ) present the same diffraction peaks characteristic of aluminum crystallized in the face-centered-cubic (fcc) structure corresponding to the file N°00-004-0787 (Figure 2).

**3.2. Morphological Characterization of Bare and Functionalized Al NPs.** Scanning electron micrographs show particles with an average size of ca. 50 nm, as displayed in Figure 3. It is noteworthy that the particles are aggregated, even after the whole functionalization procedure and the polymer coating.

In order to obtain deeper insight on the particle morphology at the individual scale, transmission electron micrographs were recorded, as displayed in Figure 4. It appears that the particles have nonspherical shapes. The oxide layer is visible as a corona of ca. 2–4 nm around the Al core. Interestingly, while the diazonium salt treatment does not bring major modifications on the TEM images compared to the bare Al NPs, the polymerization step leads to the appearance of a new layer around the NPs, which can be attributed to the PMAA polymer coating. This polymer layer appears to be smooth and homogeneous with an average thickness of around 4 nm.

**3.3. Surface Chemical Composition of Al NPs.** XPS analysis revealed strong modifications of the surface chemical composition of the hybrids after each functionalization step. In particular, the survey spectra, displayed in Figure 5, show the appearance of a new peak after treatment by the diazonium salt

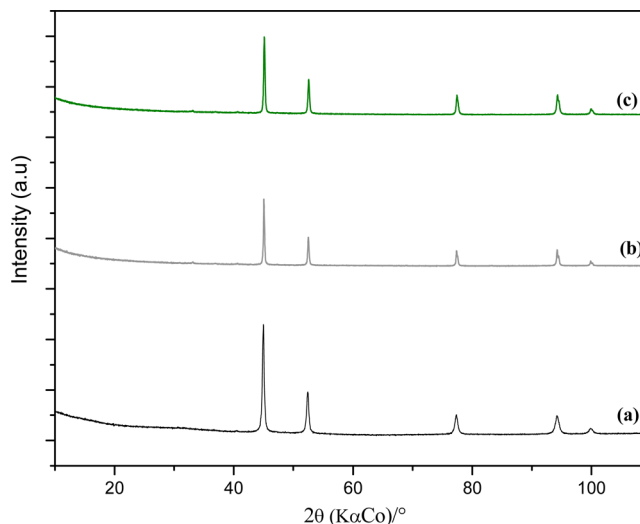


**Figure 2.** X-ray diffraction patterns of samples (a) Al, (b) Al-DEDTC, and (c) Al-PMAA $_{\text{sh}}$ .

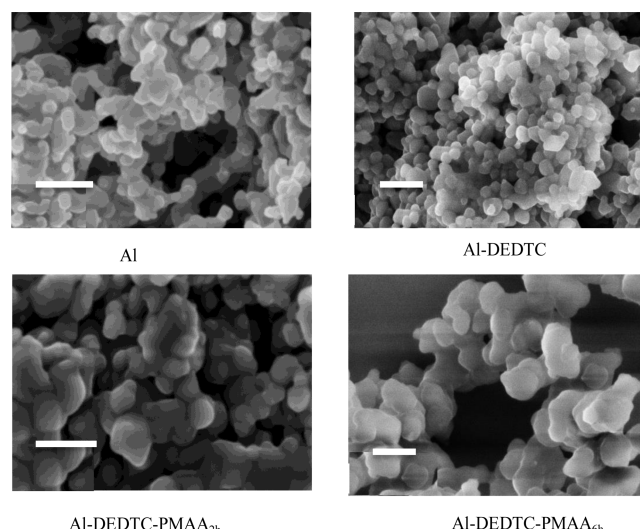


**Figure 3.** Scanning electron micrographs of bare Al, Al-DEDTC, Al-PMAA $_{2\text{h}}$ , and Al-PMAA $_{6\text{h}}$ . Scale bars = 200 nm.

due to S2p photoelectrons. Concomitantly, an attenuation of the Al2p signal compared to the C1s one is observed due to the covering of the Al core by the organic coating.

The fluorine signal results from the counterions  $\text{BF}_4^-$ , present in all samples treated by the diazonium salts. The surface elemental compositions of all the samples are summarized in Table 1. The polymerization step induces further changes with a progressive increase of the carbon content when the polymerization time increases and a concomitant decrease of the Al content. As a result, the C/Al atomic ratio increases progressively from 1.1 to 13.6, indicating an efficient coating of the Al particles by the polymer layer, the thickness of which can be controlled by the polymerization time. However, it is to note that at long reaction time (over 6 h), the polymerization seems to slow down, with Al and C atomic content remaining almost constant.

Further evidence of the presence of the PMAA layer at the surface of the Al NPs is given by the high-resolution C1s spectrum, which displays a new component C $_{\text{COOH}}$  at 289 eV (see Figure SI-1 of the Supporting Information), corresponding

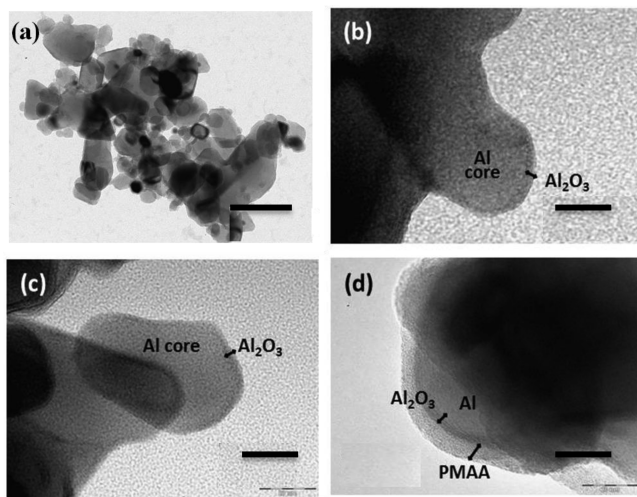


**Figure 4.** Transmission electron micrographs showing (a and b) bare Al NPs, (c) Al-DEDTC, and (d) Al-PMAA<sub>6h</sub>. Scale bar (a) = 200 nm, and scale bars (b – d) = 20 nm.

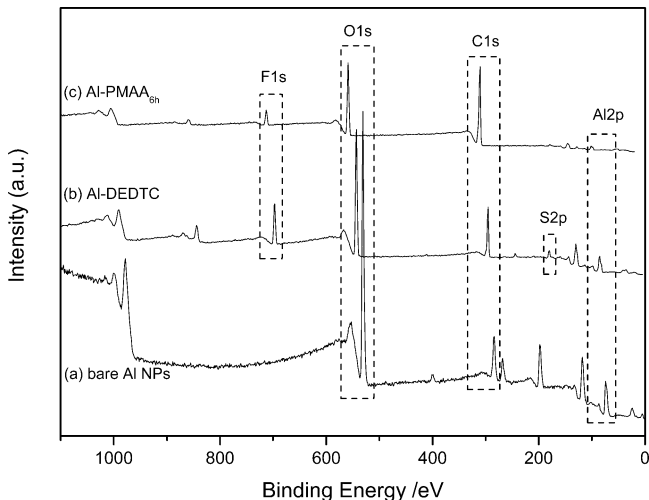


**Figure 5.** XPS survey spectra of (a) bare Al, (b) Al-DEDTC, and (c) Al-PMAA<sub>6h</sub>. For the sake of clarity, the spectra are slightly shifted along the horizontal axis.

**Table 1.** Surface Chemical Composition (Atom %) of Al NPs before and after Functionalization by the Diazonium Salt (Al-DEDTC) and Polymerization (Al-PMAA at different time)

Material	Al	C	O	F	N	S	C/Al
bare Al NPs	36	12	52	–	–	–	0.3
Al-DEDTC	23	32	33	8	1	3	1.4
Al-PMAA-2h	26	28	31	13	1	1	1.1
Al-PMAA-4h	21	39	28	10	1	1	1.9
Al-PMAA-6h	5	68	22	4	0.5	0.5	13.6
Al-PMAA-8h	6	68	22	3	0.5	0.5	11.3

to the O=C=O chemical environment. Interestingly, while the Al surface is almost completely screened by the polymer chains, the N1s and S2p signals are still detectable after 8 h of polymerization, confirming the living character of the polymerization process, leaving the DEDTC moieties at the chain extremities. In consideration of one DEDTC termination per tethered polymer chain, it is possible to estimate from the

atomic ratio 2C<sub>COOH</sub>/S a rough degree of polymerization  $D_p$ , the factor 2 being required to account for the presence of two sulfur atoms per DEDTC termination. From the  $D_p$  values (gathered in Table 4) and the molecular weight of MAA repeat units, one obtains the mean molecular weight of the chains tethered to the Al NPs, as  $M_n = D_p \times M_{MAA}$ . The plot of  $M_n$  versus polymerization time displayed in Figure 6 shows that the

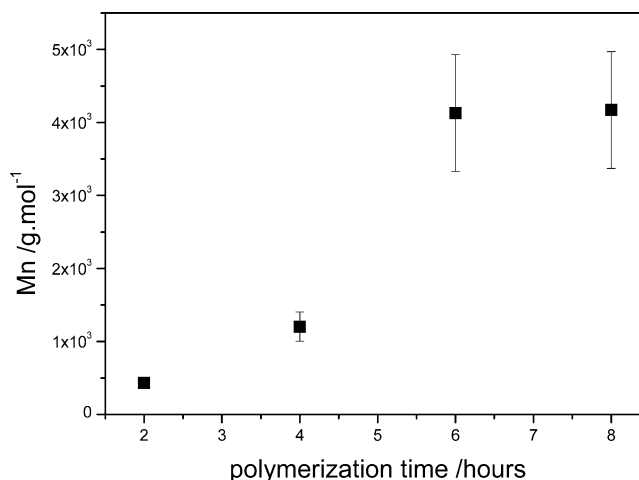


**Figure 6.** Plot of the mean molecular weight ( $M_n$ ) of the PMAA chains tethered on Al NPs versus polymerization time.

$M_n$  value increases progressively with time but saturates after 6 h of polymerization. From XPS data,<sup>12,37</sup> it is also possible to estimate the organic layer thickness (see details of the calculation in the Supporting Information). The obtained values, gathered in Table 4, show that the thickness of the PMAA grafts increase progressively with time, reaching ca. 3–4 nm after 6–8 h of polymerization, in agreement with the value estimated from TEM images.

In order to get a more precise description of the chemical nature of the Al NP/aryl layer interface, ToF-SIMS experiments were performed on model samples made of aluminum plates functionalized by the initiator  $^+N_2-C_6H_4-CH_2-S-C(=S)-N(C_2H_5)_2$ . The most significant peaks are displayed in Figure 7 and reported in Table 2.

They correspond to a large fragment or to the complete initiator linked to the aluminum surface. Interestingly, the aryl

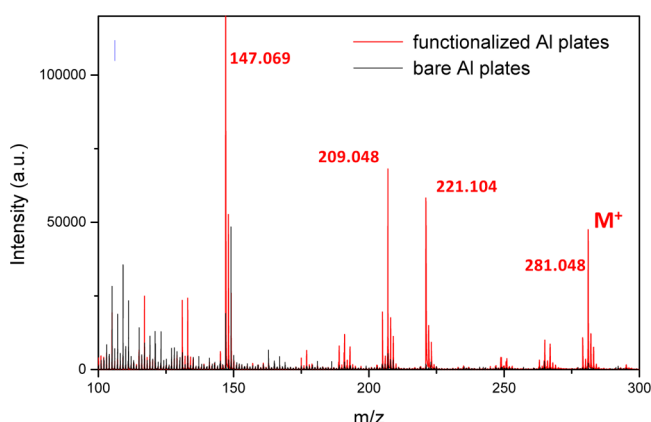


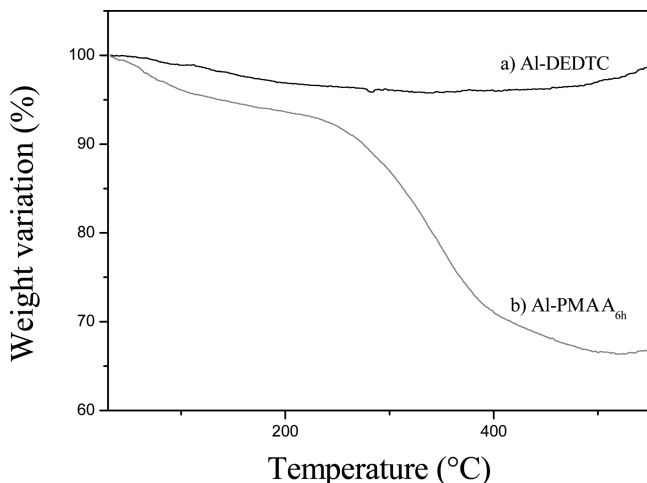
**Figure 7.** ToF-SIMS spectrum (positive ions) of an aluminum surface, untreated (black line) and modified by the diazonium salt  $^+N_2-C_6H_4-CH_2-S-C(=S)-N(C_2H_5)_2$  (red line).

**Table 2.** TOF-SIMS Spectra

experimental mass		calculated mass	molecular assignment
positive ions	negative ions		
147.069	118.957	119.008	AlO-C <sub>6</sub> H <sub>4</sub>
	149.018	147.039	AlO-C <sub>6</sub> H <sub>4</sub> -CH <sub>2</sub> -CH <sub>2</sub>
	163.062	149.000	Al-C <sub>6</sub> H <sub>4</sub> -CH <sub>2</sub> -S
209.048		162.980	AlO-C <sub>6</sub> H <sub>4</sub> -C=S
		208.968	Al-C <sub>6</sub> H <sub>4</sub> -CH <sub>2</sub> -S-C(=S)
		220.955	Al-C <sub>6</sub> H <sub>4</sub> -C=S-C(=S)-N
221.104	223.012	222.971	AlO-C <sub>6</sub> H <sub>4</sub> -CH <sub>2</sub> -S-C(=S)-N
	237.093	236.986	AlO-C <sub>6</sub> H <sub>4</sub> -CH <sub>2</sub> -S-C(=S)-N-CH <sub>2</sub>
	281.009	281.049	AlO-C <sub>6</sub> H <sub>4</sub> -CH <sub>2</sub> -S-C(=S)-N-(C <sub>2</sub> H <sub>5</sub> ) <sub>2</sub>

radicals appear to be connected to the surface mainly through Al-O-C covalent linkages, indicating that the diazonium salts react spontaneously with the oxide layer.

The presence of organics at the Al NPs surface was also evidenced by TGA carried under air flow. Figure 8 shows the

**Figure 8.** TGA of (a) Al-DEDTC and (b) Al-PMAA<sub>6h</sub>.

typical thermograms observed for all the samples. A two stages weight loss,  $\Delta m^-$ , is observed below 500 °C, due to (i) dehydroxylation and/or solvent removal and (ii) organic decomposition of DEDTC and polymer chains.

Table 3 summarizes the weight loss observed for each sample. It is very low for the sample Al-DEDTC, due to the low

**Table 3. Weight Loss Observed for the Different Samples**

samples	Al	Al- DEDTC	Al- PMAA <sub>2h</sub>	Al- PMAA <sub>4h</sub>	Al- PMAA <sub>6h</sub>
weight loss	-4.1%	-4.2%	-17.6%	-29.8%	-33.7%

molecular weight of the DEDTC molecule, and increases with the addition of MAA monomers and with polymerization time, proving the efficiency of the treatment.

From the mass fraction of the organic coating (corresponding to the weight loss observed between 200 and 500 °C), TGA can be used as a semiquantitative method for the determination of the PMAA shell thickness. Indeed, assuming a uniform coating of PMAA at the surface of Al nanoparticles, one can relate the thickness ( $x$ ) of the polymer overlayer to the main fraction of the Al core and the polymer shell using

$$x = r \times \left\{ \left[ \left( \frac{M_2 \rho_1}{M_1 \rho_2} \right) + 1 \right]^{1/3} - 1 \right\} \quad (1)$$

where  $M$  is the mass fraction,  $\rho$  the density, and  $r$  the radius of the core. The lower scripts 1 and 2 refer to Al and PMAA, respectively. The thicknesses determined by this approach vary between 1.6 nm for Al-PMAA<sub>2h</sub> to 4.3 nm for Al-PMAA<sub>6h</sub>, which compares relatively well with the values obtained by TEM and XPS.

**3.4. Passivation of the Al NPs Surface by the Organic Coating.** One key challenge for many applications of Al NPs is to avoid the formation of a thick layer of natural oxide at the surface of the NPs. This is even more crucial when the size of the NP decreases, as the surface becomes predominant with regard to the bulk. Indeed, aluminum is used in energetic materials for the high energy produced during its combustion with oxygen. The oxide layer certainly protects the Al NPs, but meanwhile, it requires supplementary energy during combustion in order to eliminate it before reaching the pure aluminum core. The covering of Al NPs by an organic coating before their contact with oxygen is a mean to decrease the fraction of oxide in the particle. In consideration of the reactivity, the coating will have low influence on the performances, the organic part being pyrolyzed at the aluminum ignition temperature (superior to 600 °C). In the energetic materials, such as propellants, it is more the nanometric size of the metallic particle which ensures a greater reactivity of the material than the actual nature of their coating.

In order to evaluate the effect of the functionalization strategy based on diazonium salts on the surface oxidation of the Al NPs, the proportion of the oxide and metallic components in the high-resolution Al2p spectra were compared for all samples. The spectra displayed in Figure 9 evidence a clear enhancement of the metallic contribution (peak at ~72 eV) relative to the oxide component (peak at ~75 eV) in the presence of the organic coating, compared to the uncoated Al NPs, indicating an effective passivation of the particle surface.

This passivation effect could be quantified through an estimation of the oxide layer thickness, from XPS data (see section 2 of the Supporting Information). The obtained values, presented in Table 4, show a decrease of ca. 57% of the oxide layer thickness after functionalization, emphasizing the efficiency of this grafting procedure to control the interfacial properties of the NPs.

## CONCLUSION

In conclusion, we have developed an efficient functionalization strategy for the grafting of functional aryl layers at the surface of

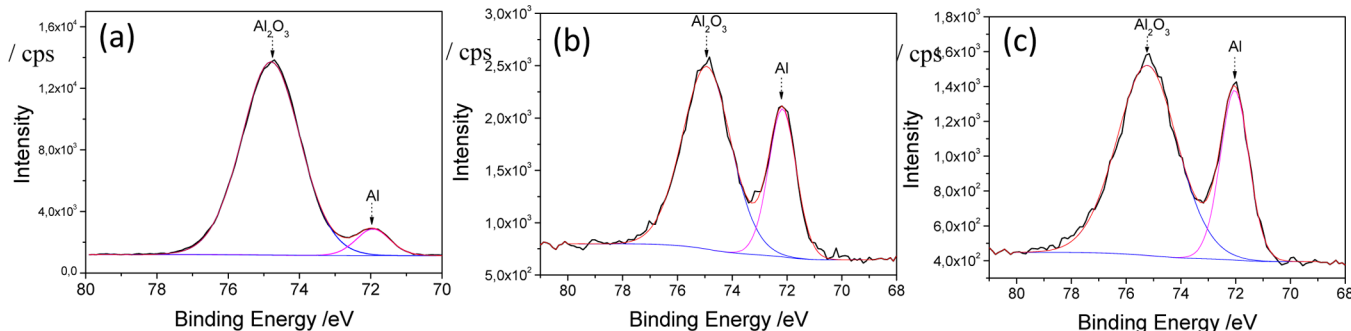


**Figure 9.** High resolution and peak fitting of Al2p spectra of (a) bare Al NPs, (b) Al-DEDTC, and (c) Al-PMAA<sub>6h</sub>.

**Table 4. Oxide Layer Thickness ( $d_{\text{Al}2\text{O}_3}$ ), Organic Layer Thickness ( $d_{\text{organic}}$ ), Degree of Polymerization ( $D_p$ ), and Mean Molecular Weight ( $M_n$ ) of the PMAA Grafts on the Surface of Al NPs**

material	$d_{\text{Al}2\text{O}_3}^a$ (nm)	$d_{\text{organic}}^a$ (nm)	$D_p$	$M_n$ (g mol <sup>-1</sup> )
bare Al NPs	4.2	—	—	—
Al-DEDTC	1.9	0.9	—	—
Al-PMAA-2h	2.0	0.8	5	430
Al-PMAA-4h	2.0	1.2	14	1200
Al-PMAA-6h	2.1	3.6	49	4100
Al-PMAA-8h	2.0	3.3	50	4200

<sup>a</sup>Estimated from XPS data (see details of the calculations in the Supporting Information). The value of  $d_{\text{organic}}$  was not calculated for bare Al NPs, although a contamination layer is present at their surface. In the case of Al-DEDTC, the value of  $d_{\text{organic}}$  accounts for the aryl layer thickness.

Al NPs. On the basis of a combination of diazonium salt chemistry and the iniferter method, we have obtained hybrid NPs, with a metallic aluminum core and a strongly anchored polymer shell. The thickness of the polymer shell could be controlled by the polymerization time, reaching 3–4 nm after 6 h of polymerization. Nevertheless, at longer polymerization time (>8h), the polymer coating does not grow any more. Interestingly, the presence of the organic coating protects the metallic Al core from oxidation, evidencing a passivation effect inferred by the grafted aryl layers that appear to be rather compact. The use of diazonium salts for modifying Al NPs opens, therefore, new opportunities for their use in various kinds of applications such as energetic materials. A direct prospect of this work will be to combine this postfunctionalization method to in situ strategies to better control the size and monodispersity of the pristine aluminum nanoparticles.

## ASSOCIATED CONTENT

### Supporting Information

XPS C1s spectra and XPS determination of oxide and organic layer thicknesses of bare and functionalized Al NPs. This material is available free of charge via the Internet at <http://pubs.acs.org>.

## AUTHOR INFORMATION

### Corresponding Authors

\*E-mail: Lorette.sicard@univ-paris-diderot.fr. Tel: 33-1-57278759. Fax: 33-01-57277263.

\*E-mail: mangeney@univ-paris-diderot.fr. Tel: +33-1-57276878. Fax: 33-01-57277263.

## Notes

The authors declare no competing financial interest.

## ACKNOWLEDGMENTS

The authors are in debt to Hélène Lecoq and Patricia Beaunier (LRS) for SEM and TEM images, respectively.

## REFERENCES

- Daniel, M. C.; Astruc, D. Gold nanoparticles: assembly, supramolecular chemistry, quantum-size-related properties, and applications toward biology, catalysis, and nanotechnology. *Chem. Rev.* **2004**, *104*, 293–346.
- Rosi, N. L.; Mirkin, C. A. Nanostructures in biodiagnostics. *Chem. Rev.* **2005**, *105*, 1547–1562.
- Zhang, P.; Sui, Y.; Xiao, G.; Wang, Y.; Wang, C.; Liu, B.; Zou, G.; Zou, B. Facile fabrication of faceted copper nanocrystals with high catalytic activity for *p*-nitrophenol reduction. *J. Mater. Chem. A* **2013**, *1*, 1632–1638.
- Xiao, G.; Zeng, Y.; Jiang, Y.; Ning, J.; Zheng, W.; Liu, B.; Chen, X.; Zou, G.; Zou, B. Synergistic modulation of surface interaction to assemble metal nanoparticles into two-dimensional arrays with tunable plasmonic properties. *Small* **2013**, *9*, 793–799.
- Brousseau, P.; Anderson, C. J. Nanometric aluminum in explosives. *Propellants, Explosives, Pyrotechnics* **2002**, *27*, 300–306.
- Tyagi, H.; Phelan, P.; Prasher, R.; Peck, R.; Lee, T.; Pacheco, J.; Arentzen, P. Increased hot-plate ignition probability for nanoparticle-laden diesel fuel. *Nano Lett.* **2008**, *8*, 1410–1416.
- Pantoya, M. L.; Granier, J. J. Combustion behavior of highly energetic thermites: Nano versus micron composites. *Propellants, Explosives, Pyrotechnics* **2005**, *30*, 53–62.
- Balazs, A. C.; Emerick, T.; Russell, T. P. Nanoparticle polymer composites: Where two small worlds meet. *Science* **2006**, *314*, 1107–1110.
- Lim, M. S.; Feng, K.; Chen, X.; Wu, N.; Raman, A.; Nightingale, J.; Gawalt, E. S.; Korakakis, D.; Hornak, L. A.; Tiperman, A. T. Adsorption and desorption of stearic acid self-assembled monolayers on aluminum oxide. *Langmuir* **2007**, *23*, 2444–2452.
- Karaman, M. E.; Antelmi, D. A.; Pashley, R. M. The production of stable hydrophobic surfaces by the adsorption of hydrocarbon and fluorocarbon carboxylic acids onto alumina substrates. *Colloids Surf., A* **2001**, *182*, 285–298.
- Taylor, C. E.; Schwartz, D. K. Octadecanoic acid self-assembled monolayer growth at sapphire surfaces. *Langmuir* **2003**, *19*, 2665–2672.
- Abel, M. L.; Watts, J. F.; Digby, R. P. The adsorption of alkoxysilanes on oxidized aluminum substrates. *Int. J. Adhes. Adhes.* **1998**, *18*, 179–192.
- Liakos, I. L.; McAlpine, E.; Chen, X.; Newman, R.; Alexander, M. Assembly of octadecyl phosphonic acid on the  $\alpha$ -Al<sub>2</sub>O<sub>3</sub> (0001) surface of air annealed alumina: Evidence for termination dependent adsorption. *Appl. Surf. Sci.* **2008**, *255*, 3276–3282.
- Spori, D. M.; Venkataraman, N. V.; Tosatti, S. G. P.; Durmaz, F.; Spencer, N. D.; Zurcher, S. Influence of Alkyl Chain Length on

- Phosphate Self-Assembled Monolayers. *Langmuir* **2007**, *23*, 8053–8060.
- (15) Crouse, C. A.; Pierce, C. J.; Spowart, J. E. Influencing solvent miscibility and aqueous stability of aluminum nanoparticles through surface functionalization with acrylic monomers. *ACS Appl. Mater. Interfaces* **2010**, *2*, 2560–2569.
- (16) Dahoumane, S. A.; Nguyen, M. N.; Thorel, A.; Boudou, J. P.; Chehimi, M. M.; Mangeney, C. Protein-functionalized hairy diamond nanoparticles. *Langmuir* **2009**, *25*, 9633–9638.
- (17) Matrab, T.; Save, M.; Charleux, B.; Pinson, J.; Cabet-Deliry, E.; Adenier, A.; Chehimi, M. M.; Delamar, M. Grafting densely-packed poly(n-butyl methacrylate) chains from an iron substrate by aryl diazonium surface-initiated ATRP: XPS monitoring. *Surf. Sci.* **2007**, *601*, 2357–2366.
- (18) Mangeney, C.; Qin, Z.; Dahoumane, S. A.; Adenier, A.; Herbst, F.; Boudou, J. P.; Pinson, J.; Chehimi, M. M. Electroless ultrasonic functionalization of diamond nanoparticles using aryl diazonium salts. *Diamond Relat. Mater.* **2008**, *17*, 1881–1887.
- (19) Mahouche Chergui, S.; Ledebt, A.; Mammeri, F.; Herbst, F.; Carbonnier, B.; Ben Romdhane, H.; Delamar, M.; Chehimi, M. M. Hairy carbon nanotube@nano-Pd heterostructures: Design, characterization, and application in Suzuki C-C coupling reaction. *Langmuir* **2010**, *26*, 16115–16121.
- (20) Mirkhalaf, F.; Paprotny, J.; Schiffrin, D. J. Synthesis of metal nanoparticles stabilized by metal–carbon bonds. *J. Am. Chem. Soc.* **2006**, *128*, 7400–7401.
- (21) Kumar, V. K. R.; Gopidas, K. R. Synthesis and characterization of gold-nanoparticle-cored dendrimers stabilized by metal–carbon bonds. *Chem.–Asian J.* **2010**, *5*, 887–896.
- (22) Ghosh, D.; Chen, S. Palladium nanoparticles passivated by metal–carbon covalent linkages. *J. Mater. Chem.* **2008**, *18*, 755–762.
- (23) Shengnan, Y.; Qinmin, P.; Liu, J. Improving the cycleability of Si anodes by covalently grafting with 4-carboxyphenyl groups. *Electrochim. Commun.* **2010**, *12*, 479–482.
- (24) Ghosh, D.; Pradhan, S.; Chen, W.; Chen, S. Titanium nanoparticles stabilized by Ti–C covalent bonds. *Chem. Mater.* **2008**, *20*, 1248–1250.
- (25) Griffete, N.; Li, H.; Lamouri, A.; Redeuilh, C.; Chen, K.; Dong, C.-Z.; Nowak, S.; Ammar, S.; Mangeney, C. Magnetic nanocrystals coated by molecularly imprinted polymers for the recognition of bisphenol A. *J. Mater. Chem.* **2012**, *22*, 1807–1810.
- (26) Griffete, N.; Lamouri, A.; Herbst, F.; Felidj, N.; Ammar, S.; Mangeney, C. Synthesis of highly soluble polymer-coated magnetic nanoparticles using a combination of diazonium salt chemistry and the iniferter method. *RSC Adv.* **2012**, *2*, 826–830.
- (27) Griffete, N.; Herbst, F.; Pinson, J.; Ammar, S.; Mangeney, C. Preparation of water-soluble magnetic nanocrystals using aryl diazonium salt chemistry. *J. Am. Chem. Soc.* **2011**, *133*, 1646–1649.
- (28) Maldonado, S.; Smith, T. J.; Williams, R. D.; Morin, S.; Barton, E.; Stevenson, K. J. Surface modification of indium tin oxide via electrochemical reduction of aryl diazonium cations. *Langmuir* **2006**, *22*, 2884–2891.
- (29) Hurley, B. L.; McCreery, R. L. Covalent bonding of organic molecules to Cu and Al alloy 2024 T3 surfaces via diazonium ion reduction. *J. Electrochem. Soc.* **2004**, *151*, B252–B259.
- (30) Pinson, J.; Podvorica, F. Attachment of organic layers to conductive or semiconductive surfaces by reduction of diazonium salts. *Chem. Soc. Rev.* **2005**, *34*, 429–439.
- (31) Belanger, D.; Pinson, J. Electrografting: A powerful method for surface modification. *Chem. Soc. Rev.* **2011**, *40*, 3995–4048.
- (32) Hinrichs, K.; Roodenko, K.; Rappich, J.; Chehimi, M. M.; Pinson, J. Aryl diazonium salts: New coupling agents. In *Polymer and Surface Science*; Chehimi, M. M., Ed.; Wiley-VCH: Weinheim, Germany, 2012.
- (33) Otsu, T.; Ogawa, T.; Yamamoto, T. Solid-phase block copolymer synthesis by the iniferter technique. *Macromolecules* **1986**, *19*, 2087–2090.
- (34) Rahane, S. B.; Kilbey, S. M.; Metters, A. T. Kinetics of surface-initiated photoiniferter-mediated photopolymerization. *Macromolecules* **2005**, *38*, 8202–8210.
- (35) de Boer, B.; Simon, H. K.; Werts, M. P. L.; van der Vegt, E. W.; Hadzioannou, G. “Living” free radical photopolymerization initiated from surface-grafted iniferter monolayers. *Macromolecules* **2000**, *33*, 349–355.
- (36) Reghunadhan Nair, C. P.; Clouet, G.; Chaumont, P. Functionalization of PMMA by a functional “iniferter”: Kinetics of polymerization of MMA using *N,N'*-diethyl-*N,N'*-bis(2-hydroxyethyl) thiuram disulfide. *J. Polym. Sci., Part A: Polym. Chem.* **1989**, *27*, 1795–1809.
- (37) Strohmeier, B. R. The effects of O<sub>2</sub> plasma treatments on the surface composition and wettability of cold-rolled aluminum foil. *J. Vac. Sci. Technol., A* **1989**, *7*, 3238–3246.